Wheat Cycle Monitoring Using Radar Data and a Neural Network Trained by a Model

Fabio Del Frate, *Member, IEEE*, Paolo Ferrazzoli, *Member, IEEE*, Leila Guerriero, Tazio Strozzi, *Senior Member, IEEE*, Urs Wegmüller, *Senior Member, IEEE*, Geoff Cookmartin, and Shaun Quegan, *Member, IEEE*

***Abstract*—This paper describes an algorithm aimed at monitoring the soil moisture and the growth cycle of wheat fields using radar data. The algorithm is based on neural networks trained by model simulations and multitemporal ground data measured on fields taken as a reference. The backscatter of wheat canopies is modeled by a discrete approach, based on the radiative transfer theory and including multiple scattering effects. European Remote Sensing satellite synthetic aperture radar signatures and detailed ground truth, collected over wheat fields at the Great Driffield (U.K.) site, are used to test the model and train the networks. Multitemporal, multifrequency data collected by the Radiometer-Scatterometer (RASAM) instrument at the Central Plain site are used to test the retrieval algorithm.**

***Index Terms*—Crops, neural networks, radar, retrieval, scattering model.**

I. Introduction

In THE LAST decades, important advances have been achieved in the agricultural applications of synthetic aperture radar (SAR). Since the 1970s, several ground-based experiments proved a significant radar sensitivity to crop parameters, and results were summarized in [1]. Further experimental studies were carried out by means of airborne SAR campaigns. Finally, the launches of the European Remote Sensing (ERS) satellites, RADARSAT, and the Japanese Earth Resources (JERS) satellites made it possible to monitor crop cycles continuously by means of spaceborne SARs [2]–[5].

In parallel, crop scattering models are being refined. Vegetation elements such as leaves, stems and ears have been represented as discrete elements and their scattering and absorption cross-sections computed by theories developed for canonical shapes, such as discs and cylinders [6]–[8]. Further developments are in progress, leading to a more detailed description of crop structure [9]–[11].

From the application point of view, the objective is to estimate the soil moisture and important vegetation variables, such as leaf area index (LAI: m^2/m^2) and biomass (kg/m^2) by means of SAR signatures. Three main steps may be identified in this process [12]: 1) to adopt a suitable radar configuration; 2) to establish a reliable relationship between the backscatter coefficient σ° and the field variables; and 3) to solve the inverse problem. As far as the first step is concerned, low frequencies, typically L-band, proved to be suitable for soil moisture monitoring, while the ERS configuration (i.e., C-band, VV polarization, 23°), in spite of its limitations, may lead to interesting results for monitoring some crops, such as wheat and rice [2], [4]. The second step is still in progress. There have been important advances, but some studies indicate that further refinements are required [2], [11]. Finally, the third step is very complex, since σ° depends on several soil and vegetation variables. Although some variables, such as the dimensions of leaves and stems, may be less interesting for applications, they still influence σ°. Therefore, inversion methods based on simple relationships between σ° and biomass (or LAI) tend to be unreliable. A more advanced approach is based on the combination of neural networks with electromagnetic models [13]–[15]. Neural networks are composed of many nonlinear computational elements (called neurons) operating in parallel and linked with each other through connections characterized by multiplying factors. This structure makes neural networks inherently suitable for addressing nonlinear problems. In contrast to methods that use empirical models, the derivation of particular rules or statistical *a priori* information on the data to be processed is not necessary in this approach. The neural network establishes the inverse mapping and the input–output discriminant relations during the training phase on the basis of data generated by the electromagnetic model.

In this paper, neural networks are adopted to retrieve soil and vegetation variables. The training is done by using a model that is based on the radiative transfer theory and combines scattering contributions by means of the matrix doubling algorithm. The model is able to compute both the backscattering coefficient (active version) and the emissivity (passive version). A detailed description of the active model foundations is given in [16]. In the same paper, the model is tested against experimental data collected at L-band over sunflower fields. In the present paper, the model is adapted to represent wheat fields, which are characterized by specific modeling problems, related to their high stem density and vertical structure [2], [11]. The model is tested against signatures collected at 5.3 GHz (C-band) by ERS-2 SAR, and trains algorithms using experimental data collected at 3.1 GHz (S-band), 4.6 GHz (C-band), and 10.2 GHz (X-band).

Manuscript received October 30, 2002; revised June 6, 2003. The data from the Great Driffield and Central Plain sites were made available in the framework of the ERA-ORA Project, funded by ECC under Contract ENV4-CT97-0465.

F. Del Frate, P. Ferrazzoli, and L. Guerriero are with the Facoltà di Ingegneria, Dipartimento di Informatica, Sistemi e Produzione (DISP), University of Rome "Tor Vergata," I-00133 Rome, Italy (e-mail: ferrazzoli@disp.uniroma2.it).

T. Strozzi and U. Wegmüller are with Gamma Remote Sensing, CH-3074 Muri BE, Switzerland (e-mail: strozzi@gamma-rs.ch).

G. Cookmartin and S. Quegan are with the Sheffield Centre for Earth Observation Science, University of Sheffield, Sheffield S3 7RH, U.K. (e-mail: s.quegan@sheffield.ac.uk).

Digital Object Identifier 10.1109/TGRS.2003.817200

As previously stated, several soil and vegetation variables influence the backscattering coefficient. A procedure based on a full inversion of all variables, assumed to evolve independently, would be too cumbersome. The retrieval procedure proposed in this paper does not lead to unmanageable numerical complexity, although the model adopted ensures a detailed electromagnetic description of the canopy. The procedure is structured into several steps, as indicated below. First of all, three wheat fields, for which detailed ground truth and ERS-2 signatures were available, are used to test the model. Then the model, using the same ground data (reference) as input, generates a set of multitemporal outputs at S-, C-, and X-band. This multitemporal dataset trains two different neural networks, to retrieve soil moisture and vegetation variables, respectively. Finally, the networks operate on radar signatures collected at a test site. The first network estimates soil moisture on a day-by-day approach. The second network, using retrieved soil moisture as input, estimates the differences between the crop cycle of the reference site and the crop cycle of the test site and, hence, the time evolution of its vegetation variables. Finally, the results are compared with ground truth measured at the test site. No *a priori* information about the test site is used in the retrieval procedure.

Inevitably, the algorithm involves some approximations, which are critically discussed in the paper. However, it has the advantage of fully exploiting the potential of multitemporal data and training the network with model outputs that consider the evolution of all vegetation variables.

Recently, a similar algorithm was tested using radiometric measurements and the passive version of the same electromagnetic model [17]. In that paper, two wheat fields were considered. Ground data from the first field were used as a reference, while radiometric data from the same field were used to test the retrieval of soil moisture and vegetation variables. Radiometric data from the second field were used to test only soil moisture retrieval, due to limitations in the available experimental data (see [17] for details). In the present paper, the retrieval procedure is tested three times using three completely independent reference datasets. Moreover, the retrieval is based on radar, instead of radiometric, signatures. This is important for applications, since the resolution of spaceborne radiometers is not sufficient for agricultural applications.

Section II describes the experimental data, collected by the ERS-2 SAR over wheat fields at the Driffield (U.K.) site and by the Radiometer-Scatterometer (RASAM) scatterometer from wheat fields in the Central Plain (CH) site. Section III describes the electromagnetic model used to train the retrieval algorithm, which is described in Section IV. Section V displays and discusses the results obtained.

II. Experiments

Two datasets are considered in this work. ERS-2 signatures collected at the Great Driffield site in 1997, as well as detailed ground truth, are used to test the electromagnetic model and train the networks. RASAM signatures and ground data collected at the Central Plain site in 1988 are used to test the retrieval procedure. Both Great Driffield and Central Plain data were made available in the framework of an ECC Concerted Action, named ERA-ORA.

In order to train the network with a multitemporal dataset of sufficiently short sampling time, ground truth collected at the Avignon site in 1993 [18] are used as an auxiliary reference.

A. Driffield Site

In 1997, several fields were monitored at the Great Driffield site by ERS-2 SAR. Only descending orbit images were considered, giving eleven images within the duration of the field campaign. These were standard ESA PRI products. Data were corrected for local incidence angles using a DEM and calibrated using the National Remote Sensing Centre, Ltd., software package TSAR. Field averaged backscattering values were extracted using a digitized map of field boundaries for the area, which had been verified on the ground. Further details are given in [2].

The important soil and vegetation variables were measured during the campaign. In particular, multitemporal signatures of three wheat fields (numbered here as 2, 3, and 5) are available. Radar data are accompanied by detailed ground truth. Vegetation variables were measured at two sites in each field. Fresh and dry biomass were measured over a representative sample of plants in each site. Soil moisture was measured by taking samples on the top 5 cm, using a can of known volume. For soil measurements, the sampling density varied from 2–12 samples per field, depending on soil conditions. Measurements covered also soil roughness, as well as dimensions and moisture of leaves, stems, and ears. Detailed information on the field measurements and satellite data are available in [2]. Some aspects that are important to the objective of the present work are summarized below.

Fig. 1 shows the temporal evolution of volumetric soil moisture content (SMC), crop biomass, LAI, and backscatter coefficient measured by ERS-2, for the three fields. It is evident that soil drying and crop growing occur almost simultaneously in springtime and early summertime. Both effects tend to decrease the backscattering coefficient. Therefore, inversion of a single parameter by means of empirical methods is not reliable, but physical models are required to isolate the different effects. For all three fields, a σ° minimum is observed at day of year (DoY) $\sim$150, followed by a slight increase in σ°. The biomass has its highest values between DoY 150 and 200.

Fig. 2 compares the trends of geometrical variables, such as leaf width, stem diameter, and ear diameter in the three fields. Although with some differences, the time evolutions in the three fields are similar. Therefore, developing retrieval algorithms based on a reference field, as it is done in this paper, appears to be a reasonable procedure. Of course, the accuracy of the algorithm will be improved if the reference and test fields are in the same climatic zone and of the same species and variety.

B. Central Plain Site

RASAM is a microwave radiometer/scatterometer system. It operated over several fields in Switzerland between 1984 and 1991. Signatures were collected at frequencies of 2.5, 3.1, 4.6, 7.2, 10.2, and 11.0 GHz, at several angles between 10° and 70°, and at VV, HH, HV, and VH polarizations [19]. Ground data covered some significant parameters such as soil moisture, soil

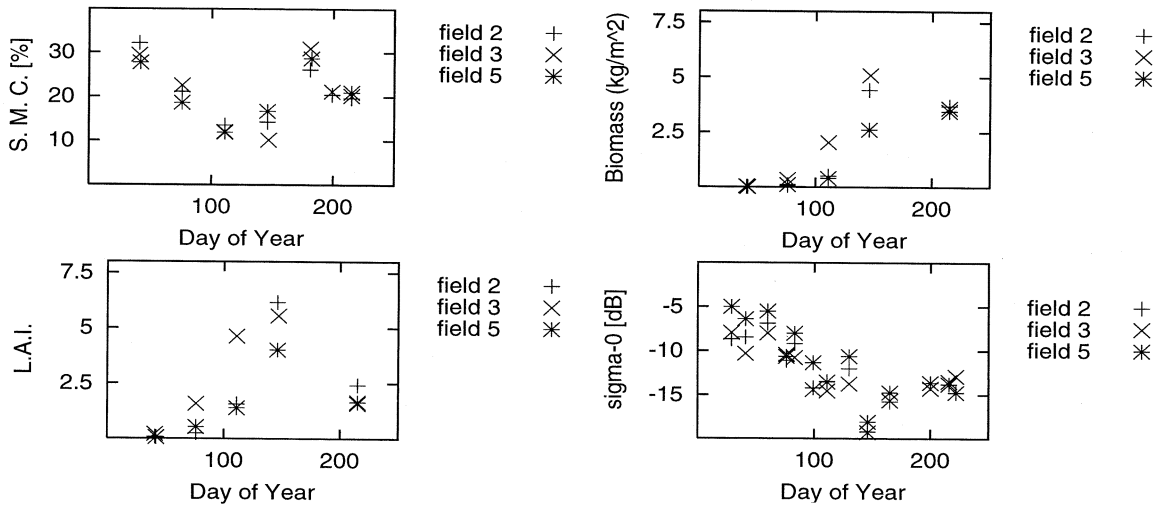

Fig. 1. Multitemporal trends of variables measured over three fields at Great Driffield. (Top left) Volumetric soil moisture content (percent). (Top right) Biomass (kilograms per square meter). (Bottom left) LAI. (Bottom right) Backscatter coefficient (decibels) measured by ERS-2 SAR.

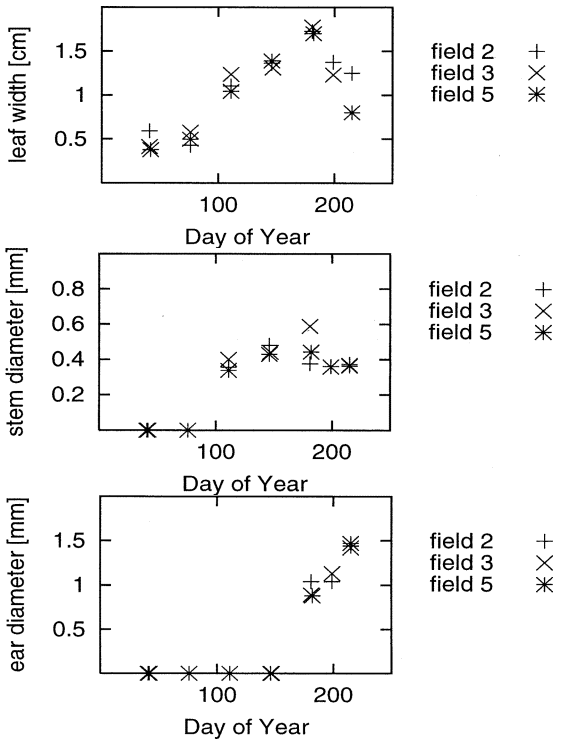

Fig. 2. Multitemporal trends of variables measured over three fields at Great Driffield. (Top to bottom) Leaf width (centimeters), stem diameter (millimeters), and ear diameter (millimeters).

roughness, crop height, crop biomass, etc. In this paper, the retrieval procedure is tested using multitemporal signatures collected over a wheat field in 1988 at the Central Plain site.

Fig. 3 shows the time evolution of soil moisture content, biomass, and σ°. Two frequency bands, i.e., 3.1 GHz (S) and 10.2 GHz (X), two polarizations, i.e., VV and HH, and an angle of 30° are selected in the figure. The SMC exceeds 0.25 m^3/m^3 during the whole period, with some limited and rapid variations observed when the crop was developed. The effects of these SMC variations on σ° are moderate at S-band, HH polarization, while they are not evident at VV polarization or X-band. As far as general σ° trends are considered, a minimum similar to the one observed in Fig. 1 for ERS is noted at S-band (particularly for VV polarization), while at X-band the trend is monotonic decreasing, except at the start of the measurements.

III. Model

The model assumes the vegetation medium to be a homogeneous half-space with rough interface, representing the soil, overlaid by an ensemble of discrete lossy scatterers, representing the plant constituents. Details of the model are given in [16], while its main aspects are summarized below.

The procedure may be subdivided into various steps.

- First of all, the bistatic scattering coefficient of soil, as well as the bistatic scattering cross sections of vegetation elements, are computed. For soil, the integral equation model [13] with an exponential correlation function, is adopted. The scatterers, which represent the plant constituents, are described as dielectric elements of canonical shape, such as discs and cylinders. For discs, representing leaves, the physical optics approximation is adopted [7]. Cylinders represent stems and ears. For these kinds of scatterers, computations are carried out assuming the internal field to be the same as that of an infinite length cylinder [8].
- The canopy is subdivided into homogeneous layers, selected in accordance with its geometrical structure. Two layers are taken for wheat. The upper layer is filled with vertical cylinders, representing ears, and discs, representing flag leaves. The lower layer is filled with thin vertical cylinders, representing stems, and discs, representing other leaves. The total number of discs per unit area is obtained as the ratio between LAI and single disc area. The fraction of discs in the upper layer (with respect to total discs) is set equal to the fraction of flag leaves (with respect to total leaves). Each layer is subdivided into several thin sublayers. For each sublayer, scattering and transmission matrices are defined, according to the procedure described in [16]. Matrix elements are related to bistatic scattering cross sections of scatterers filling

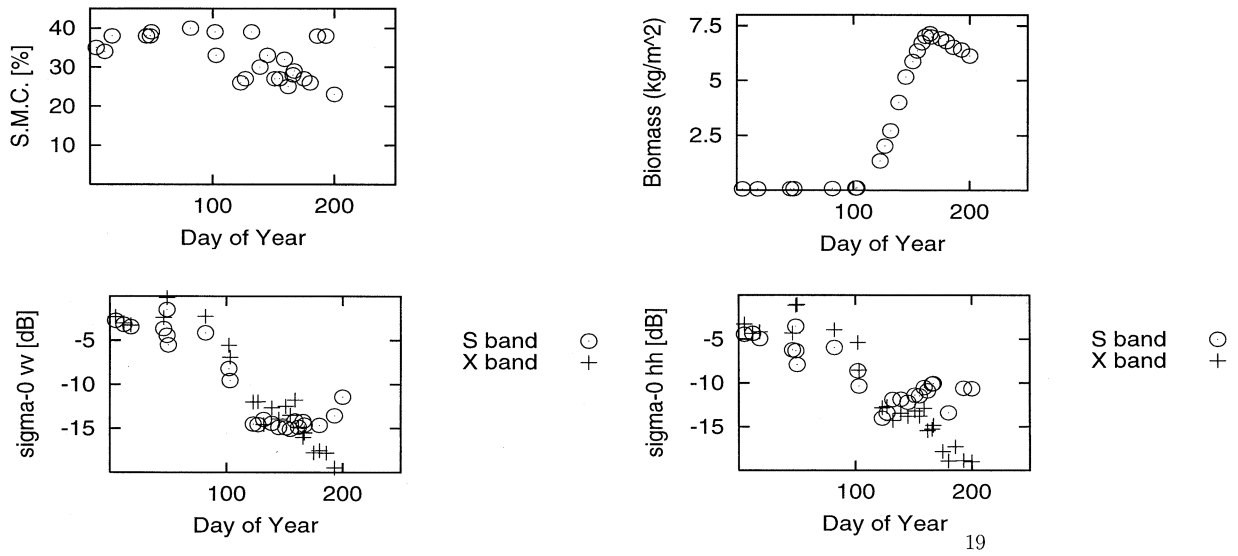

Fig. 3. Multitemporal trends of variables measured over one field at Central Plain. (Top left) Volumetric soil moisture content (percent). (Top right) Biomass (kilograms per square meter). (Bottom left) Backscatter coefficient (decibels) measured by RASAM at 30°, VV polarization. (Bottom right) Backscatter coefficient (decibels) measured by RASAM at 30°, HH polarization.

the sublayer, which must be computed for a discrete set of incidence and scattering directions. Relevant formulas are given in [16].

- For soil, a scattering matrix is defined, and its elements are computed as a function of bistatic scattering coefficient. The same angle discretization as the one adopted for the canopy, is applied. Relevant formulas are given in [16] also for this case.
- Once all the scattering and transmission matrices are available, the matrix doubling algorithm is used, under the assumption of azimuthal symmetry [13]. First of all, the algorithm is used iteratively, in order to combine the sublayer matrices and compute scattering and transmission matrices of the two layers constituting the canopy. Then, the same algorithm is used to combine the matrices of the two layers and, afterwards, to combine canopy and soil matrices. In this way, the scattering matrix of the whole soil-vegetation medium is computed.
- Finally, the backscattering coefficient is computed by means of the scattering matrix, for any required angle. The relevant formula is given in [16].

The following inputs are required by the model:

- soil permittivity;
- soil height standard deviation;
- soil correlation length;
- number of stems and ears per square meter;
- leaf area index;
- stem, ear, and leaf permittivity;
- height and diameter of stem and ear, assumed to be vertical;
- length, width, and thickness of leaves;
- orientation distribution of leaves.

Most of the data were directly available from ground truth measured at Great Driffield [2]. Soil permittivity was computed by volumetric soil moisture, using the semiempirical model described in [1]. Stem, ear, and leaf permittivities were computed by gravimetric moistures using a well-established semiempirical model [20]. No detailed information was available for leaf orientation. The Eulerian angle β of the discs was assumed to follow a $\cos^2(\beta - \beta_\circ)$ distribution, with $\beta_\circ = (3/8)\pi$. This corresponds to a predominantly erectophyle assumption, which is reasonable for wheat leaves.

Ground data collected during a previous experiment at Avignon site [18] indicated that stems and ears are partially hollow in the late season. In [18] a reduction factor, based on weight measurements, was applied to stem and ear diameters to account for this effect. A similar reduction factor was applied to Driffield data, by using a correspondence between the time development of Driffield variables and the time development of the Avignon variables [18]. Formulas used to establish this correspondence will be described in detail in Section IV.

The model was tested against ERS 2 SAR signatures measured at Driffield, since ground data at this site were sufficiently detailed to be used as inputs. Fig. 4 shows the comparison between simulated and measured backscatter coefficients for the three wheat fields. Some observations may be derived from the figures. Some discrepancies, related to surface model inaccuracies, are observed in the very early days, when the fields were essentially bare soils. The model correctly reproduces the decreasing σ° trends observed in spring and early summer, which are due to the simultaneous effects of soil drying and vegetation growth. Wheat geometry is dominated by vertical elements, such as ears and stems. At C-band, 23° and VV polarization, these mainly produce absorption of the incoming wave, associated with weak direct backscattering. A minimum is observed at ∼DoY 150, due to strong attenuation of soil backscattering, partially compensated by weak backscattering due to flag leaves and multiple interactions among leaves. In the late part of the cycle, experimental data and simulations agree in indicating a σ° increase, which is due to an increase of soil moisture and a decrease of canopy attenuation. The latter is due to vegetation drying. However, the values at the end of the cycle are lower

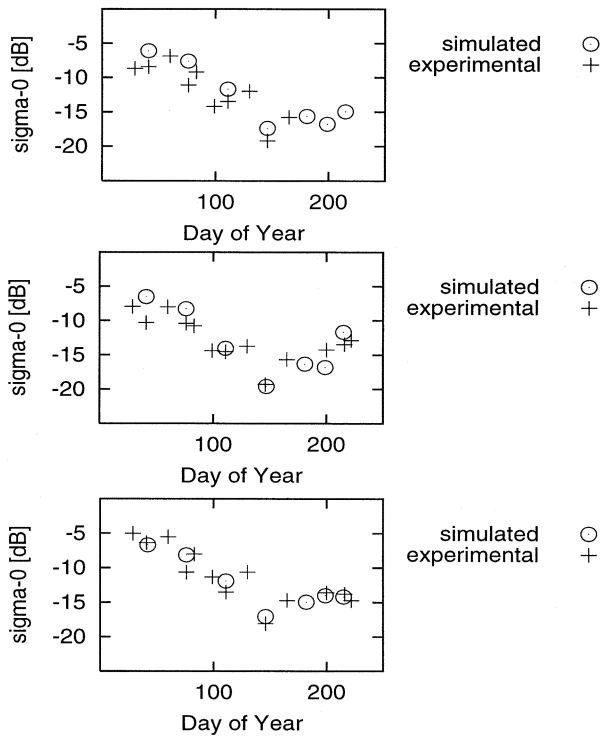

Fig. 4. Comparison between experimental and simulated multitemporal trends of backscatter coefficients (decibels) at Great Driffield. (Top to bottom) Field 2, field 3, and field 5.

than wintertime values, since a residual canopy attenuation is present.

By considering all the radar acquisitions over the three fields for which simultaneous ground truth were available, a total rms error of 2.0 dB is obtained. This error arises mainly from surface model inaccuracies in the first days of the year, when fields were bare soils.

IV. Retrieval Algorithm

This section describes two retrieval algorithms, based on neural networks trained by the model illustrated in the previous section. The neural network simulations are based on the Stuttgart University neural network simulator (SNNS).[1] The topology is formed by a multilayer perceptron with two hidden layers, while a sigmoid function is applied as the activation function of the network units [21]. The general aspects of the procedure are presented before dealing with its application to our specific sites.

A. General Aspects

A reference site, for which a multitemporal set of detailed ground data is available, must be selected for training the neural network. For each Day of Year of the reference site (DoY_R), the model is run to simulate σ°'s at the required frequencies, polarizations, and angles. Vegetation inputs are given by the ground data measured at the reference site. Moreover, computations are carried out for various situations of soil moisture and soil height standard deviations. Correlation length is dealt with by averaging over soil scattering matrices computed for a realistic range between 3 and 8 cm. We also introduce a "density factor" F_d in the computations, to allow for simulation of σ°'s for fields with a different number of plants per square meter (N) than that at the reference site (N_R). The density factor is defined as $F_d = N/N_R$.

In summary, for a given reference site and for each radar configuration (i.e., for each required set of frequencies, polarizations and angles), the model generates an output file containing simulated σ°'s for the following scenarios:

- volumetric soil moisture: from 0.05–0.4 $\mathrm{m}^3/\mathrm{m}^3$, step 0.01 $\mathrm{m}^3/\mathrm{m}^3$;
- soil height standard deviation: 0.5 and 1 cm;
- vegetation variables taken from datasets measured for each DoY_R;
- $F_d = 0.5, 1, 1.5$.

The total number of simulated samples is 61 746.

1) Soil Moisture Retrieval: First of all, soil moisture is retrieved. A first neural network is adopted, which reverses the role of inputs and outputs with respect to the model. In the training phase, the input–output pairs of the σ°'s computed by the model and the corresponding values of soil moisture are used to compute the neural network coefficients. The latter establish a correspondence between σ°'s and soil moisture values, in a simulated scenario of no *a priori* knowledge about vegetation status and soil roughness. In the test phase, the soil moistures corresponding to the dates of the radar measurements at the test site are considered as unknowns to be retrieved. A set of measured σ°'s (at the same frequency, polarizations and angles as those of the training phase) is fed to the trained network, giving the estimated soil moistures as outputs. The network shows n input nodes, corresponding to σ°'s measured at the n radar configurations used. The hidden nodes are processing units and one output node gives the retrieved soil moisture. The retrieval is performed by the same network for all days with radar data available at the test site.

2) Vegetation Variables Retrieval: As previously stated, the model generates a set of simulated σ°'s, covering several DoYs and several conditions of the soil variables and F_d at the selected frequencies, polarizations, and angles. The basic concept of the retrieval procedure is to assume that other fields of the same crop type will have a similar growth cycle, but shifted in time and/or with different duration. That is, if $Y_R(\mathrm{DoY}_R)$ represents the trend of a vegetation variable throughout the reference field crop cycle, we assume that the following expression holds for a vegetation variable Y of a generic field of the same crop

$$Y(\mathrm{DoY}) = F_d \cdot Y_R(\mathrm{DoY}_R). \tag{1}$$

The correspondence between the two time scales is established by an inverse relationship such as

$$\mathrm{DoY}_R = \mathrm{DoY}_{R0} + b + a \cdot (\mathrm{DoY} - \mathrm{DoY}_{R0}). \tag{2}$$

DoY is a generic day of a field growth cycle, and DoY_{R0} is selected in a central location of the reference field cycle. a is the factor which modifies the width of the time trend, and b the parameter which modifies the time location of the cycle.

[1]http://www-ra.informatik.uni-tuebingen.de/SNNS/

Several time series of backscattering coefficients are simulated by varying a, b, and F_d within realistic ranges. The simulated time series, in conjunction with the corresponding values of a, b, and F_d, are then used to compute the network coefficients. As a result of the training phase, multitemporal sets of backscatter coefficients are associated with crop cycles which may differ from the reference cycle in crop density, and also in temporal location and temporal duration. At this stage, the soil moisture values retrieved by the first network are used.

After the training phase, the retrieval procedure is tested at a test site. A multitemporal set of σ°'s measured at the same frequencies, polarizations and angles as those of the training phase, is taken.

As far as vegetation parameters are considered, the network, using experimental σ°'s as input, estimates the differences between the multitemporal ground data for the test field and those for the reference field. The outputs provided by the network are the F_{dT} factor (where the T denotes "test"), and the pair of parameters a_T and b_T containing information about the temporal evolution of the test cycle. Vegetation variables at the test site may be computed as a function of a_T, b_T, and F_{dT} according to the procedure indicated below.

Let Y_T be the value of a vegetation variable to be retrieved for a given Day of Year at the test site (DoY_T). Some variables, such as biomass and LAI, are dependent on density; in this case we have

$$Y_T(\mathrm{DoY}_T) = F_{dT} \cdot Y_R(\mathrm{DoY}_R) \tag{3}$$

with

$$\mathrm{DoY}_R = \mathrm{DoY}_{R0} + b_T + a_T \cdot (\mathrm{DoY}_T - \mathrm{DoY}_{R0}). \tag{4}$$

Other variables, such as dimensions and moisture of leaves, stems, and ears are not dependent on the density. For these variables, formula (3) is modified to

$$Y_T(\mathrm{DoY}_T) = Y_R(\mathrm{DoY}_R) \tag{5}$$

while formula (4) is not modified. In this way, all vegetation variables may be estimated for the whole test cycle.

The proposed algorithm may be a step toward a complete solution of the retrieval problem. In the model adopted here, the backscattering coefficient is influenced by: soil moisture, surface height standard deviation and correlation length, number of plants per square meter, dimensions and moistures of leaves, stems, and ears, and leaf orientation distribution, for a total of 14 variables. The number is even higher in models adopting multiscale surface representations and/or coherent approaches. A direct mathematical inversion of such a large system of relationships is extremely difficult. On the other hand, methods based on simple relationships between σ° and a single variable are heavily influenced by the specific properties of the adopted datasets. The adopted algorithm is based on a complete model simulation, including all variables influencing σ°, without leading to an unmanageable retrieval procedure.

B. Specific Issues Concerning the Dataset

For both soil moisture and vegetation variables, the procedures described above were applied three times, using each of the three wheat fields at the Great Driffield site taken as reference. The wheat field in the Central Plain site was taken as the test site.

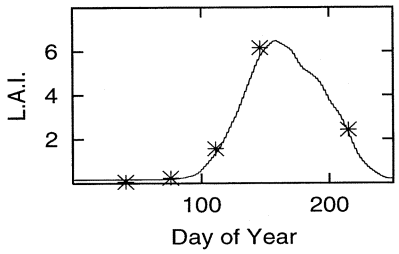

Fig. 5. Multitemporal trend of LAI over field 2 at Great Driffield. (Asterisks) Measured. (Continuous line) Interpolated.

Seven temporal samples of ground truth were available for the whole crop cycle at Great Driffield. This number of samples was not sufficient since the procedure for vegetation variable retrieval needs simulated data with a short sampling time. In order to overcome this problem, the Great Driffield data were interpolated with the aid of ground truth measured at Avignon in 1993 [18], used as an auxiliary reference. Avignon ground measurements were carried out with short sampling time (three days on average). Moreover, after further processing, vegetation variables were provided for every DoY during the crop cycle. A first processing, based on (1) and (2), was applied to the time trend of variables measured at Avignon. In this way, for each variable used as a model input, data measured at Great Driffield were fitted. An example of the procedure is shown in Fig. 5, where LAI samples measured at Great Driffield are compared with a continuous trend obtained following the interpolation procedure.

In the neural network training phase, the model was run for every DoY_R using interpolated values of the vegetation variables as input. To generate the time series necessary to train the network, we used (1) and (2), letting a vary in the range 0.5–2, b in the range -20 to 20, and the density factor F_d in the range 0.5–1.5.

V. Results

The method illustrated in Section IV was tested using RASAM signatures from a wheat field in the Central Plain site. For each of the two retrieval processes, i.e., soil moisture and vegetation variables, we selected a set of radar configurations suitable for the given application, using diverse information sources, but avoiding the introduction of too many nodes in the network.

For soil moisture we selected: 3.1 GHz, HH and VV, 20° and 30°. The topology of the network is 4-10-10-1. The learning phase was limited to less than 20 min. The procedure described in Section IV-A1 yielded three multitemporal sets of retrieved soil moistures, each corresponding to one selected reference field. The three retrieved multitemporal trends of soil moistures are compared with that measured at the test site in Fig. 6. The three comparisons show similar properties. In the time interval from $\mathrm{DoY}_R = 41$ to $\mathrm{DoY}_R = 102$, the soils were bare and wet. The measured soil moisture was close to 0.4 $\mathrm{m}^3/\mathrm{m}^3$, with

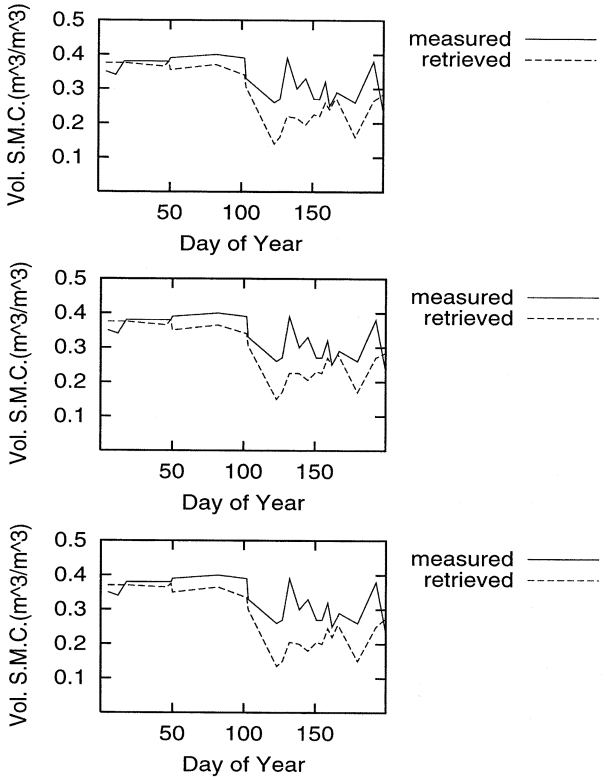

Fig. 6. Multitemporal trends of volumetric soil moisture content (m^3/m^3). (Top to bottom) Field 2 as reference, field 3 as reference, and field 5 as reference. (Continuous line) Measured over the test field. (Dashed line) Retrieved by the algorithm.

very limited variations. The retrieved soil moistures are high and stable, although slightly underestimated. After $\mathrm{DoY}_R = 102$ the field was affected by two main effects: slight drying and rapid vegetation growth (see Fig. 3). In this time interval, the algorithm is unable to reproduce soil moisture trends. This is due to the effect of vegetation, which causes the radar signal to become insensitive to soil moisture variations. Fig. 3 shows that the backscatter coefficients were scarcely influenced by variations in soil moisture. This is also related to the high density of the test field, which showed a maximum biomass of more than 7 kg/m^2 (see again Fig. 3). In [17], better results were achieved for vegetation covered soils, but L-band signatures were also available; the instrument had a different sensitivity, since it was passive, and biomass values were lower. By taking only samples from $\mathrm{DoY}_R = 41$ to $\mathrm{DoY}_R = 102$ the following rms soil moisture errors were computed:

- reference field 2: 0.0285 m^3/m^3;
- reference field 3: 0.030 m^3/m^3;
- reference field 5: 0.0305 m^3/m^3.

For vegetation variable retrieval, we selected: 3.1, 4.6, and 10.2 GHz, HH and VV, and 30° for eight days. The DoY_{R0} parameter of formula (4) was set to 170.
In this case, the topology of the network is 48-35-20-3. Less then 20 min were sufficient to get the network trained also in this case. The procedure described in Section IV yielded the following values.

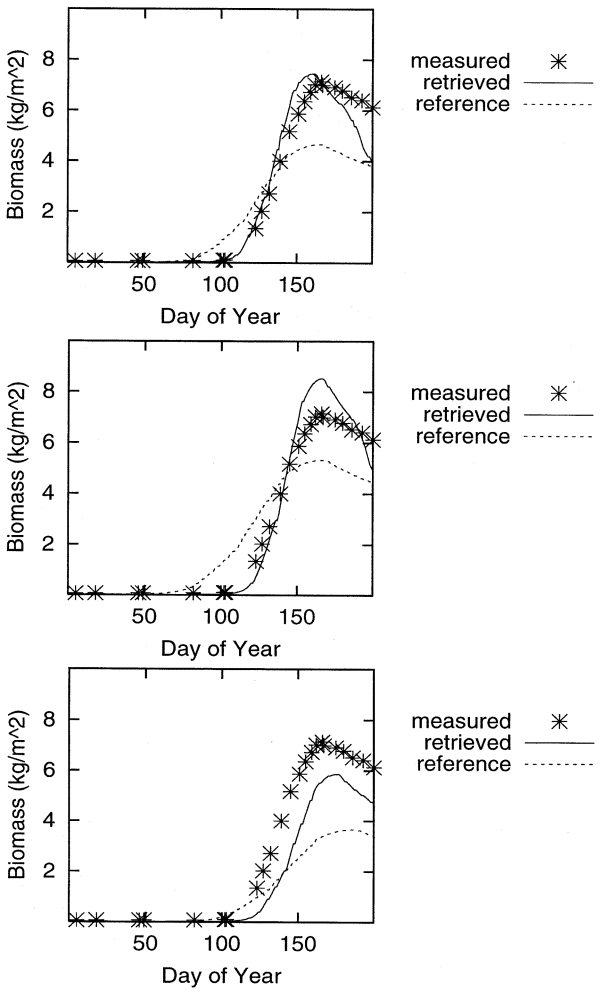

Fig. 7. Multitemporal trends of biomass (kg/m^2). (Top to bottom) Field 2 as reference, field 3 as reference, and field 5 as reference. (Crosses) Measured over the test field. (Continuous line) Retrieved by the algorithm. (Dashed line) Measured over the reference field.

- For reference field 2

$$a_T = 1.63 \quad b_T = 11 \quad F_{dT} = 1.6.$$

- For reference field 3

$$a_T = 1.88 \quad b_T = 4 \quad F_{dT} = 1.6.$$

- For reference field 5

$$a_T = 1.65 \quad b_T = 8 \quad F_{dT} = 1.6.$$

Ground data measured at the test site were not used in the retrieval procedure, but were used to test the final results. Fig. 7 compares the biomass trends measured at the test field and those obtained by applying (3) and (4) to the biomass trends measured at the three reference sites, respectively. Also, for sake of comparison, the biomass trends measured at the reference sites are shown. In all three cases, the time locations of retrieved trends match that measured, although those of the reference sites were appreciably different. Some discrepancies, up

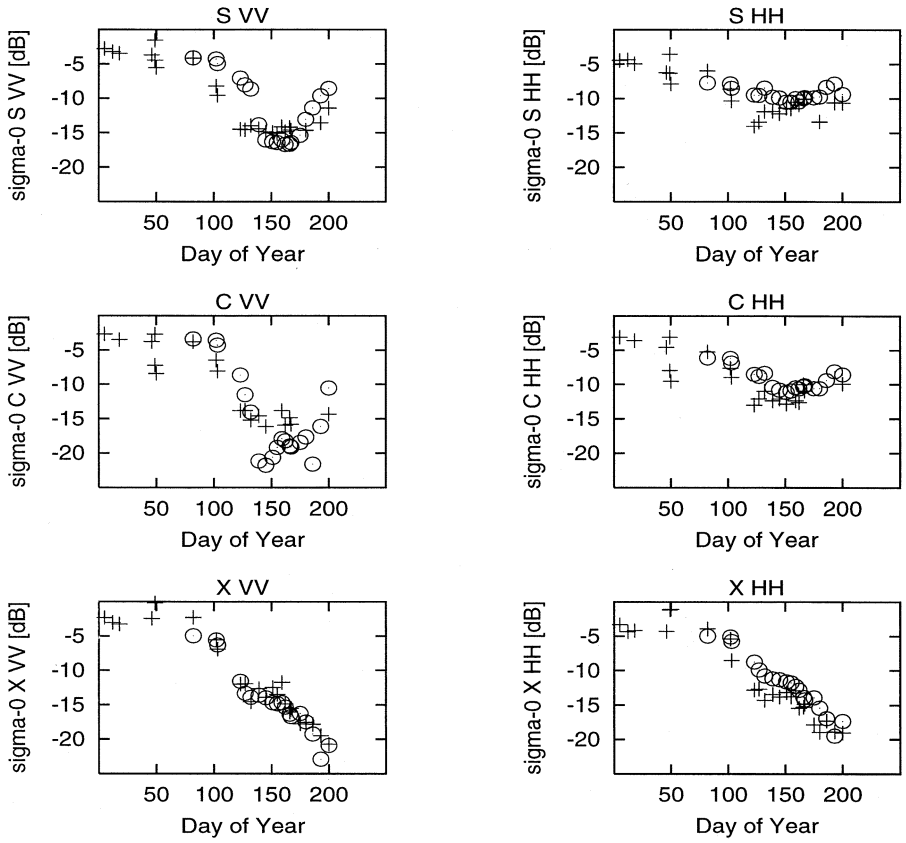

Fig. 8. Comparison between experimental backscatter coefficients (decibels) measured at (crosses) Central Plain and (circles) values obtained as a result of the retrieval procedure. (Left) VV polarization. (Right) HH polarization. (Top to bottom) S-, C-, and X-band.

to about 1.5 kg/m^2, are observed in the maximum values, especially when fields 3 and 5 are taken as reference. This is explained by the presence of a saturation effect, which causes the backscattering coefficient to become insensitive to biomass variations when the biomass is high. The problem has been discussed in several previous papers (e.g., see [12]). The test field was dense, with a maximum biomass higher than 7 kg/m^2. The algorithm estimates high F_d values for all three cases, but the precision of this estimate was reduced by saturation. In spite of this problem, the algorithm produces a significant shift toward the measured biomass trend, although the reference trends are quite different from it in all three cases. It must also be noted that a completely "blind" procedure was adopted. Retrieved data were obtained using only data from reference sites and a theoretical model, without using any *a priori* information about the test field.

Fig. 8 compares measured σ°'s with values generated by the model for the same frequencies, polarizations, angles and soil variables as the test site: the time series of σ°'s has been obtained using the retrieved F_{dT} value and after application of the transformation given by formula (4) to the time cycle of reference field 2. Underestimations of σ° are observed at C-band VV for some time intervals. This problem was already observed in other works [2], where it was attributed to overestimation of the attenuation at VV. This is also shown in [22], in which it is stated that the sparse medium approximation may not be appropriate for wheat, so that the attenuation cannot be estimated accurately by the optical theorem. However, in Fig. 8 the correspondence is generally good. The model is able to reproduce the general frequency and polarization properties described in Section 2.2. Moreover, a matching between multitemporal σ° trends is produced by the application of the algorithm, as described in Section 4.1.

VI. Conclusion

An algorithm is proposed for retrieving soil moisture and the multitemporal evolution of the properties of wheat crops, based on ground truth from a reference field, a scattering model and neural networks. The algorithm takes the evolution of all vegetation variables into account, yielding a retrieval process which is fast and convenient. S-, C-, and X-band radar signatures are used.

The accuracy of soil moisture retrieval is fair when the soil is bare, but is reduced under developed vegetation. The availability of lower frequencies (i.e., L-band) signatures would have mitigated this problem.

As far as vegetation is concerned, the algorithm reproduces the biomass trend with reasonable agreement, although the absolute accuracy is reduced by saturation effects.

In a future operational context, the retrieval procedure could be improved by also using L-band, when available, and planning the campaigns in such a way as to have a reference field with the same general properties as those of the fields to be monitored (e.g., same variety, same climatic conditions, etc.).

This work is aimed at proposing and testing general algorithms. Future research should analyze the potential of single radar configurations.

ACKNOWLEDGMENT

The data from the Avignon test site were kindly made available by J.-P. Wigneron (INRA, France).

REFERENCES

[1] F. T. Ulaby, R. K. Moore, and A. K. Fung, *Microwave Remote Sensing: Active and Passive—Vol. III*. Dedham, MA: Artech House, 1986.

[2] G. Cookmartin, P. Saich, S. Quegan, R. Cordey, P. Burgess-Allen, and A. Sowter, "Modeling microwave interactions with crops and comparison with ERS-2 SAR observations," *IEEE Trans. Geosci. Remote Sensing*, vol. 38, pp. 658–670, Mar. 2000.

[3] P. Saich and M. Borgeaud, "Interpreting ERS SAR signatures of agricultural crops in Flevoland, 1993–1996," *IEEE Trans. Geosci. Remote Sensing*, vol. 38, pp. 651–657, Mar. 2000.

[4] F. Ribbes and T. Le Toan, "Rice field mapping and monitoring with RADARSAT data," *Int. J. Remote Sens.*, vol. 20, pp. 745–765, 1999.

[5] A. Rosenqvist, "Temporal and spatial characteristics of irrigated rice in JERS-1 L-band SAR data," *Int. J. Remote Sens.*, vol. 20, pp. 1567–1587, 1999.

[6] H. J. Eom and A. K. Fung, "A scatter model for vegetation up to K_u-band," *Remote Sensing Environ.*, vol. 19, pp. 139–149, 1984.

[7] D. M. Le Vine, R. Meneghini, R. H. Lang, and S. S. Seker, "Scattering from arbitrarily oriented dielectric disks in the physical optics regime," *J. Opt. Soc. Amer.*, vol. 73, pp. 1255–1262, 1983.

[8] M. A. Karam and A. K. Fung, "Electromagnetic scattering from a layer of finite length, randomly oriented, dielectric, circular cylinders over a rough interface with application to vegetation," *Int. J. Remote Sens.*, vol. 9, pp. 1109–1134, 1988.

[9] N. S. Chauhan and R. H. Lang, "Radar backscattering from alfalfa canopy: A clump modeling approach," *Int. J. Remote Sens.*, vol. 20, pp. 2203–2220, 1999.

[10] T. Chiu and K. Sarabandi, "Electromagnetic scattering from short branching vegetation," *IEEE Trans. Geosci. Remote Sensing*, vol. 38, pp. 911–925, Mar. 2000.

[11] J. M. Stiles and K. Sarabandi, "Electromagnetic scattering from grassland—Part I: A fully phase-coherent scattering model," *IEEE Trans. Geosci. Remote Sensing*, vol. 38, pp. 339–348, Jan. 2000.

[12] P. Ferrazzoli, "SAR for agriculture: Advances, problems and prospects," in *Proc. 3rd Int. Symp. Retrieval of Bio- and Geophysical Parameters from SAR Data for Land Applications*, Sheffield, U.K., Sept. 2001, ESA SP-475, pp. 47–56.

[13] A. K. Fung, *Microwave Scattering and Emission Models and Their Applications*. Norwood, MA: Artech House, 1994.

[14] Y. Q. Jin and C. Liu, "Biomass retrieval from high-dimensional active/passive remote sensing data by using artificial neural networks," *Int. J. Remote Sens.*, vol. 18, pp. 971–979, 1997.

[15] F. Del Frate and L. F. Wang, "Sunflower biomass estimation using a scattering model and a neural network algorithm," *Int. J. Remote Sens.*, vol. 22, pp. 1235–1244, 2001.

[16] M. Bracaglia, P. Ferrazzoli, and L. Guerriero, "A fully polarimetric multiple scattering model for crops," *Remote Sensing Environ.*, vol. 54, pp. 170–179, 1995.

[17] F. Del Frate, P. Ferrazzoli, and G. Schiavon, "Retrieving soil moisture and agricultural variables by microwave radiometry using neural networks," *Remote Sensing Environ.*, vol. 84, pp. 174–183, 2003.

[18] P. Ferrazzoli, J.-P. Wigneron, L. Guerriero, and A. Chanzy, "Multifrequency emission of wheat: Modeling and applications," *IEEE Trans. Geosci. Remote Sensing*, vol. 38, pp. 2598–2607, Nov. 2000.

[19] U. Wegmüller, "Signature research for crop classification by active and passive microwaves," *Int. J. Remote Sens.*, vol. 14, pp. 871–883, 1993.

[20] M. A. El Rayes and F. T. Ulaby, "Microwave dielectric spectrum of vegetation—Part I: Experimental observations," *IEEE Trans. Geosci. Remote Sensing*, vol. 25, pp. 541–549, 1987.

[21] C. M. Bishop, *Neural Networks for Pattern Recognition*. New York: Oxford Univ. Press, 1995.

[22] G. Picard, T. Le Toan, F. Mattia, A.-M. Gatti, F. Posa, A. D'Alessio, C. Notarnicola, and E. Sabatelli, "A backscatter model for wheat canopies. Comparison with C-band multiparameter scatterometer measurements," in *Proc. 3rd Int. Symp. Retrieval of Bio- and Geophysical Parameters from SAR Data for Land Applications*, Sheffield, U.K., Sept. 2001, ESA SP-475, pp. 291–296.

Fabio Del Frate (M'03) received the laurea degree in electronic engineering and the Ph.D. degree in computer science, both from the University of Rome "Tor Vergata," Rome, Italy, in 1992 and 1997, respectively.

From September 1995 to June 1996, he was a Visiting Scientist with the Research Laboratory of Electronics, Massachusetts Institute of Technology, Cambridge. In 1998 and 1999, he was with the ESRIN Center, European Space Agency, Frascati, Italy, as a Research Fellow and was engaged in projects concerning end-to-end remote sensing applications. Currently, he is a Full Researcher of University of Rome "Tor Vergata," where he teaches a course of electromagnetic pollution and is involved in research programs on electromagnetics and remote sensing.

Paolo Ferrazzoli (M'95) graduated from the University of Rome "La Sapienza," Rome, Italy, in 1972.

In 1974, he joined Telespazio S.p.A., Rome, Italy, where he was mainly active in the fields of antennas, slant-path propagation, and advanced satellite telecommunication systems. In 1984, he joined University of Rome, "Tor Vergata," Rome, Italy, where he is presently working, teaching microwaves and propagation. His current research is focused on microwave remote sensing of vegetated terrains, with particular emphasis on electromagnetic modeling. He has been involved in international experimental remote sensing campaigns such as AGRISAR, AGRISCATT, MAESTRO-1, MAC-Europe, and SIR-C/X-SAR. He has participated with the coordinating team of the ERA-ORA Project, funded by ECC, establishing an assemblage among several European researchers working in radar applications. He is a member of the Science Advisory Group of the European Space Agency SMOS Project.

Leila Guerriero received the laurea degree in physics from the University of Rome "La Sapienza," in 1986, and the Ph.D. degree in electromagnetism from the University of Rome "Tor Vergata," Rome, in 1991.

Since 1994, she has been a permanent researcher at the University of Rome, "Tor Vergata," where she is now holding a course on satellite monitoring. Her research activities at "Tor Vergata" are mainly concerned with modeling microwave backscattering and emissivity from agricultural and forested areas. In 1988, she was involved in a cooperation between the Jet Propulsion Laboratory, Pasadena, CA, and the Italian National Research Council for investigations on geophysical applications of imaging spectrometry in infrared and visible remote sensing. In 1995, she participated in a European Space Agency (ESA) project concerning radiometric polarimetry of the sea surface. In 1999–2001, she participated at the ECC concerted action ERA-ORA whose objective was to improve radar data analysis and utilization. More recently, she has been involved in the ESA project on the Soil Moisture and Ocean Salinity satellite.

Tazio Strozzi (M'98–SM'03) received the M.S. and Ph.D. degrees from the University of Bern, Switzerland, in 1993 and 1996, respectively, both in physics.

He has been with Gamma Remote Sensing, Muri, Switzerland, since 1996, where he is responsible for the development of radar remote sensing applications and is manager of a number of research and commercial projects. From 1996 to 1998, he was a part-time Physics Teacher at the Highschool of Bellinzona, Bellinzona, Switzerland. From 1999 to 2001, he worked as a part-time Visiting Scientist at the University of Wales, Swansea, U.K. He is Principal Investigator for ERS, ENVISAT, and JERS projects on forest mapping and subsidence monitoring. His current activities include SAR and SAR interferometry for landuse applications (including forest, urban areas, and hazard mapping) and differential SAR interferometry for subsidence monitoring, glacier motion estimation, and landslide surveying.

Urs Wegmüller (M'94–SM'03) received the M.S. and Ph.D. degrees from the University of Bern, Bern, Switzerland, in 1986 and 1990, respectively, both in physics.

Between 1991 and 1992, he was a Visiting Scientist at the Jet Propulsion Laboratory, California University of Technology, Pasadena, working on the retrieval of canopy parameters from microwave remote sensing data. Between 1993 and 1995, at the University of Zürich, Zürich, Switzerland, his research included interferometric data processing, theoretical modeling of scattering in forest canopies, and retrieval algorithm development for geo- and biophysical parameters using SAR interferometry. In 1995, he was a founding member of GAMMA Remote Sensing AG, Muri, Switzerland, which is active in the development of signal processing techniques and remote sensing applications. As CEO of GAMMA, he has overall responsibility for GAMMA's activities. In addition, he is directly responsible for a number of research and commercial projects of GAMMA. His main involvement currently is in the development of applications and the definition and implementation of related services in land surface deformation mapping, hazard mapping, landuse mapping, and topographic mapping. He is Principal Investigator for ERS, ENVISAT, SRTM, and ALOS announcement of opportunity projects on SAR and SAR interferometry-related calibration issues, application development, and demonstration.

Geoff Cookmartin received the B.A. degree in electrical sciences from Trinity College, Cambridge, U.K., in 1981, and the M.S. degree in biophysics and bioengineering from the University of London, London, U.K., in 1983.

He was a Researcher in medical physics and subsequently in climate modeling before joining the Sheffield Centre for Earth Observation Science, Sheffield, U.K., where he worked on modeling and direct measurements of radar interaction with agricultural crops.

Shaun Quegan (M'90) received the B.A. and M.S. degrees in mathematics from the University of Warwick, Coventry, U.K., in 1970 and 1972, respectively, and the Ph.D. degree from the University of Sheffield, Sheffield, U.K., in 1982.

From 1982 to 1986, he was a Research Scientist with the Marconi Research Centre, Great Baddow, U.K., and led the Remote Sensing Applications Group from 1984 to 1986. He established the SAR Research Group at the University of Sheffield in 1986, whose success led to his Professorship awarded in 1993. In the same year, he helped to inaugurate the Sheffield Centre for Earth Observation Science, of which he remains the Director. In 2001, he became the Director of the U.K. National Environmental Research Council Centre for Terrestrial Carbon Dynamics (CTCD). This multiinstitutional center is concerned with assimilating earth observation and other data into process models of the land component of the carbon cycle. His broad interests in the physics, systems, and data analysis aspects of radar remote sensing are now subsumed in the more general aim of exploiting EO technology to meet the needs of the CTCD.